Characteristics of acoustic mode gravity waves on the ground and their effect in the ionosphere

*Toshihiko Iyemori[1], Yoko Odagi[1], Shigeo Sugitani[2], Yasuharu Sano[3], Hiroyuki Shinagawa[2], Toshimitsu Ohno[4], Yoshikazu Tanaka[5], Masahito Nose[1], Masato Iguchi[6], Hiroyuki Hashiguchi[7], Yoshihiro Yokoyama[1], Tadashi Aoyama[1], Kunihito Nakanishi[1], Vijak Pangsapa[8]

1. Graduate School of Science, Kyoto University, 2. National Institute of Information and Communications Technology (NICT), 3. Asahi University, 4. Shimonano-Sato, Niyodogawa-cho, 5. Kyoto University, 6. DPRI, Kyoto University, 7. RISH, Kyoto University, 8. Faculty of Science, Chulalongkorn University

Short period waves from lower atmosphere generate small-scale field-aligned currents through ionospheric dynamo. The magnetic fluctuations with amplitude about 1 nT and spatial scale about 100 –200 km generated by the small-scale field-aligned currents were named as “magnetic ripples”. The most plausible source of the atmospheric waves is the cumulus convection. Although the global distribution and its local time or seasonal variation of the amplitude of magnetic ripples strongly suggest the cumulus convection as the main origin, we need to clarify what mode of atmospheric waves contributes to the magnetic ripples and what meteorological condition correspond them. For those purposes, we analyze ground based magnetic and micro-barometric variations. We try to make quantitative estimation of the contribution from both acoustic and internal mode of gravity waves, acoustic resonance, etc.

The followings are our tentative results:

・Averaged PSD (power spectral density) increases to longer period (at least to 30 minute).

・PSD of pressure has a bulge in a range of acoustic gravity mode waves (100 –400 sec)

・The amplitude of the bulge is highly variable around vertical resonance period.

・PSD is larger on dayside.

・Average location of PSD peaks show slight shift depending on the latitude and season.

Keywords: micro-barometric variation, acoustic mode gravity waves, ionospheric current, vertical acoustic resonance

Relationship between magnetic ripples observed by the Swarm satellites and lower atmospheric disturbances

*Tadashi Aoyama[1], Toshihiko Iyemori[1], Kunihito Nakanishi[1]

1. Graduate School of Science, Kyoto University

The Swarm satellites, which are the low Earth, polar orbiting satellites, observed small-amplitude (0.1–5 nT) magnetic fluctuations, so-called magnetic ripples (MRs), with period around a few tens of seconds along the satellite orbit in the topside ionosphere at middle and low latitudes. A possible generation mechanism of the MRs is as follows. (1) The atmospheric waves generated by the lower atmospheric disturbance propagate to the ionospheric layer. (2) The neutral wind perturbations caused by the atmospheric wave drive the ionospheric layer dynamo, so that Hall and Pedersen currents flow in the ionosphere. (3) Because the dynamo region is limited, directions of the dynamo electric fields in the two adjoining dynamo regions with the spatial scales of the neutral wind perturbation apart are opposite. Therefore the ionospheric currents diverge to flow along the geomagnetic field-line with much higher conductivity. (4) As an Alfvén wave with polarized electric field, the front of the current circuit propagates along the geomagnetic field-line to the conjugate point on the ionosphere. (5) The currents are closed to make an electric current circuit which is made up of the currents in the ionosphere and field-aligned currents (FACs). The MRs are the spatial structure of small-scale FACs, and we confirmed with the Swarm observations their basic characteristics to be almost the same with those obtained by the CHAMP satellite. That is, the global distribution of the averaged MR amplitudes has clear geographical, seasonal and local time dependence highly correlated with the ionospheric conductivities. We found that the averaged amplitudes of the MRs derived from the Swarm-B satellite which flies about 50 km higher altitude are slightly smaller than those of the Swarm-A and -C, suggesting that the location of origin of the MRs is below ~470 km altitude, i.e., not in the magnetosphere. From the global distribution and its characteristics, the source of the MRs has been expected to be the atmospheric waves generated by lower atmospheric disturbances including the effects of earthquakes or volcanic eruptions. The fact that the MRs appear almost always suggests that some typical meteorological phenomena are the main source of MRs. To confirm the suggestion, we tried to find the connection between the MRs and typhoons as the first step. To show the evidence which correlates the MRs with typhoons, we performed an event and a statistical analyses with track data of typhoons. The data of 54 typhoons during the period from 26 November 2013 to 31 July 2016 are used for the statistical analysis. The results show that the averaged amplitudes of the MRs during typhoon activity are, in general, except for the day side local time sector, larger than those during non-typhoon condition. The event analyses indicate amplitudes enhancement of the MRs around the typhoons, and the latitude of the enhancement moved with the typhoon. These analyses indicate that typhoons are one of the source meteorological phenomena of the MRs. From the comparison with the infrared brightness temperature data the convection activity include typhoon seems to affect the amplitude of MRs. These results indicate that the MRs are generated by the lower atmospheric waves through the ionospheric dynamo.

Keywords: Magnetic ripple, Magnetic fluctuation, Field-aligned current, Ionospheric dynamo, Acoustic gravity wave, Swarm

Ionospheric disturbances associated with volcanic eruptions observed by GPS-TEC and HF Doppler sounding

*Aritsugu Chonan[1], Hiroyuki Nakata[1], Hiroyo Ohya[1], Toshiaki Takano[1], Ichiro Tomizawa[2], Takuya Tsugawa[3], Michi Nishioka[3]

1. Graduate School of Engineering, Chiba University, 2. The University of Electro–Communications, 3. National Institute of Information and Communications Technology

It is reported that ionospheric disturbances are caused not only by solar-terrestrial conditions but the phenomena below the ionosphere such as earthquakes, typhoons and volcanic eruptions. Compared with ionospheric disturbances caused by earthquakes, there are very few studies examining the ionospheric disturbances associated with volcanic eruptions.
In this study, we have examined ionospheric disturbances associated with volcanic eruptions using GPS-TEC and HF Doppler sounding. We detected ionospheric disturbances associated with Mt. Asama eruption at 11:02 UT on Sep., 1st, 2004. In HF Doppler sounding observation, the spiky disturbances whose frequency is about 7 - 16 mHz was observed firstly. Following this disturbances, longer-period disturbance was appeared, whose frequency is about 3 - 5 mHz. The former disturbance was also observed by GPS-TEC,
whose ionospheric pierce points were located near the Mt. Asama. From the propagation time of this disturbance, it is possible that the eruption generated shock waves which propagated to the higher ionosphere. In terms of the frequency, the latter disturbances observed by HFD sounding shows the resonance of the atmospheric wave between the lower ionosphere and the ground.

Keywords: Ionosphere, GPS-TEC, HF Doppler

Long-term variation of geomagnetic Sq filed and its cause

*Masahiko Takeda[1]

1. Data Analysis Center for Geomagnetism and Space Magnetism, Graduate School of Science, Kyoto University

Long-term variation of geomagnetic Sq field was used to study that of neutral pressure difference of the thermosphere (PD), considering high correlation between Ampere force by geomagnetic Sq currents and PD. It was shown that long term variation of PD can be explained almost only solar activity variation. Other factors such as eletric conductivity and geomagnetic main filed will be considered in the presentation.

Keywords: geomagnetic daily variation, long term variation, solar activity, pressure difference in the thermosphere, electric conductivity, geomagnetic main field strength

Bimodal electron energy distribution observed by sounding rocket in the Sq current focus

*Takumi Abe[1]

1. Japan Aerospace Exploration Agency, Institute of Space and Astronautical Science, Department of Solar System Sciences

“S-310-44” sounding rocket experiment was conducted on January 15, 2016 to investigate electron heating and anomalous phenomena occurring in the Sq current focus. A total of 5 instruments to measure electron energy distribution, electric field, magnetic field, and plasma wave were installed on this rocket to observe key parameters for elucidating the physical process responsible for the electron heating. We reported last year that the electron temperature was observed to be about 200 K larger than the background temperature at 100-110 km altitude in the Sq current focus. In this presentation, we will talk about a result of our recent analysis on the electron energy distribution obtained during the rocket flight.
Fast Langmuir Probe (FLP), which is one of the onboard instruments, is capable of measuring electron energy distribution with a cylindrical probe based on Druyvesteyn method. In this measurement, it is possible to estimate electron energy distribution from the second derivative of the probe current with respect to the applied voltage once the space potential can be determined on the rocket. The space potential corresponds to the voltage where the second derivative of the probe current has a sharp minimum.
The FLP Data obtained in the region below 100 km altitude show ordinary energy distribution of ionospheric electrons by which the electron temperature and density are calculated from the gradient in the electron deceleration region and the space potential. In contrast, it becomes difficult to determine a position of the space potential in the altitude range between 100 and 110 km. Moreover, bimodal peaks in the second derivative are found to exist in the higher energy from the space potential above 110 km altitude. A possible cause of such bimodal energy distribution will be 1) Bi-Maxwellian energy distribution with two different temperatures, 2) Electron temperature anisotropy, and 3) Two distributions consisting of stational ionospheric electrons and higher energy electrons coming from different altitude. In addition, another characteristics of the observed energy distribution is that the peak height of the second derivative has a periodic variation according to the phase of rocket spin, which may be related to the cause of such a distribution. We also need to discuss a causal relationship between the high electron temperature in 100 –110 km altitudes and these higher-energy electrons. In this talk, we will present the latest result of our analysis of the electron energy distribution.

Keywords: Sq current system, Electron energy distribution, Souding rocket, Electron heating

Variations in the D-region heights during the total solar eclipse of 9 March 2016 in Insonesia using AVON data

*Hiroyo Ohya[1], Kyohei Miyama, Fuminori Tsuchiya[2], Hiroyuki Nakata[1], Kozo Yamashita[3], Yukihiro Takahashi[4]

1. Graduate School of Engineering, Chiba University, 2. Planetary Plasma and Atmospheric Research Center, Graduate School of Science, Tohoku University , 3. Salesian Polytechnic, 4. Graduate School of Science, Hokkaido University

We report increase in the reflection heights of LF transmitter signals during a total solar eclipse in Indonesia on 9 March, 2016, using AVON (Asia VLF Observation Network) data. The transmitter signals of JJY-Fukushima (FKS, 40 kHz), JJY-Saga (SAG, 60 kHz), and BPC (China, 68.5 kHz) were received at Pontianak (PTK), Indonesia, where the maximum magnitude of the solar eclipse was 0.929 at 00:25 UT. The magnitude of the solar eclipse at the transmitter sites was about 0.2. The all paths did not cross the eclipse path. During the solar eclipse (00:00 –01:30 UT), the average changes of the phase delay of the SAG-PTK and BPC-PTK paths were 40º and 42º, respectively. Assuming a usual daytime height for the LF waves to be 70 km, the phase delays on both the SAG-PTK and BPC-PTK paths correspond to the increase in the reflection heights of about 1.5 km based on the Earth-ionosphere waveguide mode theory. The LF intensity of the FKS-PTK path during the solar eclipse was slightly larger by about 6.5 dB than that before and after the eclipse time. The increase in the LF reflection heights suggests the decrease in the D-region electron density during the solar eclipse.

Modeling of Na airglow emission and first results on the nocturnal variation at midlatitude

*Mallepula Venkata Sunil Krishna[1], Tikemani Bag[1,2]

1. Indian Institute of Technology Roorkee, 2. Physical Research Laboratory, Ahmedabad

The ablation of meteors at the mesopause region results in the formation of sodium layer. Due to the fact that it has a large scattering cross section and also that it acts as a tracer for the thermal and dynamical states of the atmosphere in the mesosphere region, the mesospheric sodium has been studied extensively among the meteoric metals. A model for sodium airglow emission is developed by incorporating all the known reaction mechanisms. The neutral, ionic and photochemical mechanisms are successfully implemented into this model. The values of reaction rate coefficients are based upon the theoretical calculations as well from experimental observations. The densities of major species are calculated using the continuity equations, whereas for the minor, intermediating and short lived species steady state approximation method is used. The modeled results are validated with the rocket, lidar and photometer based observations for a branching ratio of 0.04. The inputs have been obtained from other physics-based models and ground- and satellite-based observations to give the combined volume emission rate (VER) of Na airglow between 80 and 110 km altitude. In the present study, the model is used to understand the nocturnal variation of Na VER during the solstice conditions. The model results suggest a variation of peak emission layer between 85 and 90 km during summer solstice condition, indicating a lower value of peak emission rate during summer solstice. The emission rates bear a strong correlation with the O3 density during summer solstice, whereas the magnitude of VER follows the Na density during winter solstice. The altitude of peak VER shows an upward shift of 5 km during the winter solstice.

Keywords: mesospheric sodium, meteor ablation, ozone, modeling of atmosphere, mesospheric chemistry

Improvement of 3D analysis of ionospheric plasma density over Japan

*Ryo Mizuno[1], Mamoru Yamamoto[1], Susumu Saito[3], Akinori Saito[2]

1. Kyoto University Research Institute for Sustainable Humanosphere, 2. Department of Geophysics Faculty of Science, Kyoto University, 3. Electronic Navigation Research Institute Navigation System Department

Real-time monitoring of the ionospheric plasma distribution is important for the correction of the measurement errors of satellite navigation. We developed three-dimensional ionosphere tomographic analysis with GEONET data, and have started the real-time analysis since April 1, 2016. The purpose of this study is to improve this 3D tomography analysis. There are two points to be improved in this system. The first point is analysis of the whole GOENET data. The data before April 1, 2016 is not analyzed yet. We will analyze the archived GEONET data by using the supercomputer KDK at Kyoto University. Then the analysis results will be open to the public from a web page. The other point is improvement of graphic display of the tomography results. We now have four limited methods to show analysis results. To show distribution of the plasma density at different angles, we developed the vertical display along any azimuthal direction designated by a pair of horizontal locations (longitude and latitude). We plan to improve the web data service including these points.

Preliminary results of the ionospheric observation by new ionosondes, VIPIR2

*Michi Nishioka[1], Hisao Kato[1], Masayuki Yamamoto[1], Seiji Kawamura[1], Takuya Tsugawa[1], Mamoru Ishii[1]

1. National Institute of Information and Communications Technology

National Institute of Information and Communications Technology (NICT) has been observing ionosphere by ionosondes for over 60 years in Japan. At present, four ionosondes at Wakkanai (Sarobetsu), Kokubunji, Yamagawa, Okinawa (Ogimi) are automatically operated and controlled from Tokyo. Ionospheric parameters such as foF2 and foEs are automatically scaled from the ionograms. The scaled parameters are provided through our web site (http://wdc.nict.go.jp/IONO/) and used for monitoring ionospheric disturbances. Currently we are replacing the current 10C type ionosondes with Vertical Incidence Pulsed Ionospheric Radar 2 (VIPIR2) ionosondes. VIPIR2 ionosonde can separate the O- and X-modes of ionospheric echoes automatically using an antenna array, which would make it easy and successful to scale the ionogram automatically. As of 2016, hardware of VIPIR2 ionosonde are installed at the four stations and its observation has started. Arrival directions of ionospheric echo were also estimated with the phase measurements of the antenna array. In the presentation, preliminary results of the VIPIR2 observation will be shown and possible collaborations will be discussed.

Keywords: ionosonde, VIPIR2, HF radar

Study of equatorward-extending structures of ionospheric irregularity using GPS-TEC in Northern America

*Toshiki Sugiyama[1], Yuichi Otsuka[1], Takuya Tsugawa[2], Michi Nishioka[2]

1. Institute for Space-Earth Environmental Research, Nagoya University, 2. National Institute of Information and Communications Technology

There are about 2700 dual-frequency GPS receivers in Northern America. The GPS receivers provide the data of carrier phase and pseudo-range measurements at two frequencies every 30 seconds. Phase and group velocities of the GPS signals are advanced and delayed, respectively, by electrons in the ionosphere. So the Total Electron Content (TEC) along the entire line-of sight (LOS) between receiver and satellite can be derived by analyzing the GPS data.
We used the Rate of TEC change Index (ROTI) to detect the ionospheric irregularities. ROTI is the standard deviation of Rate of TEC change (ROT) in 5 minutes, and ROT is the changes of TEC in 30 seconds. The two dimensional maps of ROTI can be obtained from all available GPS data in North America. For projecting ROTI on the two dimensional map, we assume that there is the ionized single layer at altitude of 300 km. The spatial resolution is 0.75 ˚×0.75 ˚in latitude and longitude.
A magnetic storm occurred on 17 March 2015. It started at 05 UT, and Dst index reached a minimum of -223 nT at 23 UT. Enhancement of ROTI were seen at 09:00-11:00 UT and 21:00-24:00 UT. The ROTI enhancement region observed at 09-11 UT was consistent with auroral region observed from DMSP satellites. At 21-24 UT, Storm Enhanced Density (SED) was seen from absolute TEC map, and ROTI enhancement was observed in SED and poleward region of SED.
Equatorward-extending structures of ROTI enhancement region were seen at 09:00-10:30 UT and 13:00-15:30 UT in equatorward of auroral region, northern latitude of 40-50 degrees. The scale of the Equatorward-extending structures were about 150 km in the parallel direction. We calculated the drift velocity of plasma in east-west and north-south direction from data of HF radar at Christmas valley (43.27 ˚N, -120.36 ˚E) using least squares method. The enhancement of eastward drift velocity were seen at 09-11 UT and 12-14 UT and the drift velocity were about 500m/s. In this study, we examine the relationship between the fine structures of ROTI enhancements and plasma drift.

Keywords: Ionosphere, TEC, GPS, ROTI

Observations of ionospheric scintillation and total electron content using Global Navigation Satellite System (GNSS) receivers in Tromsø, Norway

*Sayaka Sakamoto[1], Yuichi Otsuka[1], Yasunobu Ogawa[2], Keisuke Hosokawa[3]

1. Nagoya University, 2. National Institute of Polar Research, 3. University of Electro-Communications

In the terrestrial ionosphere, electron density irregularities may cause variations of signal strength and/or carrier phase in trans-ionospheric satellite transmission signals received on the ground, which are commonly called ionospheric scintillations. Scintillations are categorized into amplitude scintillations and phase scintillations. Amplitude scintillations are observed as fluctuations of the signal strength, which are caused by interference between signals diffracted by irregularities. The amplitude scintillations are normally quantified by S_4 index, which is standard deviation of the received power normalized by its mean value. Phase scintillations are detected as high frequency fluctuations in the carrier phase, which are caused by variations in the refractive index due to spatial and temporal variations in electron density. The phase scintillations are normally quantified by σ_ϕ index, which is the standard deviation of the carrier phase. Phase scintillations occur both in equatorial and polar regions. In contrast, it is known that the amplitude scintillations in the equator are larger than those in the polar region.
In this study, GPS scintillations at high latitude were compared and analyzed using dual frequency (L1 : 1575.42 MHz and L2 : 1227.60 MHz) Global Navigation Satellite System(GNSS) receivers in Tromsø, Norway. This measures the amplitude and phase of the received signals at a sampling frequency of 50Hz for each satellite and calculates scintillation indices. In the present study, phase scintillations are monitored by estimating ROTI (Rate of TEC change Index). ROTI is the standard deviation of ROT (Rate of TEC change), where ROT is differential of the TEC time-series. In previous studies, amplitude scintillations are remarkable in high latitude, however we observed weak amplitude scintillations at high latitude by using low noise receivers in this study. We researched seasonal variations of S_4 and ROTI from the measurement data for the last three years, from January 2013 to December 2015. Both S_4 and ROTI have larger values at night mainly in spring and summer, and their occurrence rates depend on the season and local time. These features indicate that, at night in winter in the polar region, irregularities exist in the polar cap patches from the dayside area across the central polar cap, while electron density becomes uniform due to ionizations by solar radiation in summer. However, the S_4 increases do not always coincide with the ROTI increases. Therefore, we compared increases of S_4 and ROTI on daily basis. In this study, we classified the S_4 and ROTI data into three cases and compared them: simultaneous increase of S_4 and ROTI, increase of only S_4 and increase of only ROTI. The simultaneous increase occurs mainly in the morning and daytime. the increase of either S_4 or ROTI is mainly in the nighttime. Duration of S_4 increases tends to be longer than that of ROTI. Moreover, only ROTI increase in the daytime of summer. In this work, we considered generation mechanisms of the ionospheric irregularities which result in scintillations in the polar region.

Keywords: GPS scintillation, ROTI, Ionospheric irregularities

Study of thermospheric wind variations at substorm onsets using a Fabry-Perot interferometer at Tromsoe, Norway

*Heqiucen XU[1], Kazuo Shiokawa[1], Shin-ichiro Oyama[1], Yuichi Otsuka[1]

1. Institute for Space-Earth Environmental Research, Nagoya University

We studied the thermospheric wind variations at the onsets of isolated substorms by using a Fabry-Perot interferometer (FPI) at Tromsoe, Norway. The wind variations were measured from the Doppler shift of both red line (630.0 nm, altitudes: 200-300 km) and green line (557.7 nm, altitudes: 90-100 km) emissions with a time resolution of ~13 min. The wind data were obtained for 7 years from 2009 to 2015. We first identified the onset times of local isolated substorms by using ground-based magnetometer data of Tromsoe and Bear Island stations, and then checked the wind variations before and after these onset times. Totally, we obtained 8 events from red line data and 10 events from green line data located at different local times. By checking the all-sky images at Tromsoe, we found that most wind observations were made at the equatorward of substorm onset arcs at the onset times. For half of the events, the observation location kept at the south of the auroral arcs from -30 min to +90 min of the event times. Then, we calculated the differences of wind velocities at the onset time and at 30-min (1-hour) after the onset time using winds averaged over ±15 min (±30 min) of the epoch time. For red line events, except for few notable decreases at dawnside, eastward wind tends to increase from the onset time to both 30-min and 1-hour after the onset time at all nightside local times. This result is opposite to the tendency expected from thermospheric tidal wind variations, and suggest a particular eastward drive of thermospheric wind during substorms. With some exceptions, northward wind tends to decrease at local times before 2 LT and increase after that, which is consistent with the expectation from thermospheric tides. For green line events, eastward components have a tendency of increase at all local times with some notable decreases at duskside. Northward components show some increases at pre-midnight sector, and significant decreases at duskside, post-midnight sector and dawnside. All the observed wind changes after the substorm onsets were less than 76 m/s for red line events, and 51 m/s for green line events. These wind changes are much smaller than the typical plasma convection speed, indicating that the plasma motion caused by thermospheric wind through ion-neutral collision is a minor effect as the driver of high-latitude plasma convection and as the triggering of substorm onset. Since the movement of onset arcs could inevitably affect the local wind field, we will consider this factor when discussing the wind variations in the presentation.

Keywords: Thermospheric wind, Substorm, Fabry-Perot interferometer

Spatial and temporal variations of upper mesospheric winds inferred by using successive images of noctilucent clouds observed in Iceland.

Ryoma Yamashita[1], *Hidehiko Suzuki[1]

1. Department of physics, Meiji university

Injection of momentum through dissipations of gravity waves propagated from lower atmosphere and active productions of minor constituents caused by precipitation of energetic particles are known as dominant sources of disturbances in upper mesosphere. Since some of these disturbances occur locally and intermittently, it is important to know time constant (i.e. diffusivity) against such impulsive fluctuations on momentum and concentration of minor constituents to understand the energy and mass budgets in the upper mesosphere. One of the straight methods to know the amplitude of the eddy diffusion is to measure the spatial distribution of wind field with high temporal resolution. In this study, derivation of spatial and temporal variation of upper mesospheric winds by tracking a motion of noctilucent cloud (NLC) observed by a ground-based color digital camera in Iceland is conducted. The procedure for wind field estimation consists with 3 steps; (1) projects raw images to a geographical map (2) enhances NLC structures by using FFT method (3) determines horizontal velocity vectors by applying template matching method to two sequential images. In this talk, a result of the wind derivation by using successive images of NLC with 3 minutes interval and ~1.5h duration observed on the night of Aug 1st, 2013 will be reported as a case study.

Keywords: Noctilucent cloud, wind field, mesopause, upper mesosphere

Development of the electron density automatic estimation algorithm in the ionosphere lower region

*Taketoshi Miyake[1], Ryota Nakazawa[1], Yuki Ashihara[2]

1. Department of Informatic system, Faculty of Engineering, Toyama Prefectural University, 2. National Institute of Technology, Nara College

In the lower ionosphere, the approximate electron density profile can be estimated from the comparison between these observation results obtained by sounding rocket and propagation caracteristics calculated with Full wave method. This estimation process, which is so-called ” wave absorption method”, has some problems. At first, we have no clear standard for comparing observation results and propagation characteristics calculated with Full wave method. In addition, we have to iterate many times correcting the electron density profile by handwork, calculating propagation characteristics with Full wave method and comparing observation results and calculated propagation characteristics. This iteration takes too long to estimate appropriate electron density profile. To reduce these problems, we developed an application to realize automated estimation of electron density profile by analyzing radio wave propagation characteristics.
In the previous study, they succeeded to estimate accurate electron density profile in the ionosphere automatically in very short time. In the estimated electron density profile, however, there was an unnatural sudden fluctuation of the electron density in low-altitude region. We improverd the estimation algorithm and succeeded to estimate natural electron density profile automatically.

Keywords: ionospheric lower region, Full-wave method, altitude profile of electron density

Difference between North-South and East-West components of ELF magnetic disturbances associated with lightning detected at Kawatabi, Osaki, Miyagi, Japan

*Tomoko Nakagawa[1], Syota Takahashi[1], Kotaro Nishiyama[1]

1. Information and Communication Engineering, Tohoku Institute of Technology

In the record of 0.1-20 Hz Extremely Low Frequency (ELF) magnetic variations observed by using two sets of induction magnetometers for NS and EW components, there found cases where broadband disturbances were present only in one of the two components. Intense disturbance was found in EW component in 6 out of 8 events found at Kawatabi, in the absence of NS disturbances. It would suggest the orientation of the source lightning near the observation site.

Keywords: ELF, lightning, magnetic variation, East-West, induction magnetometer, direction

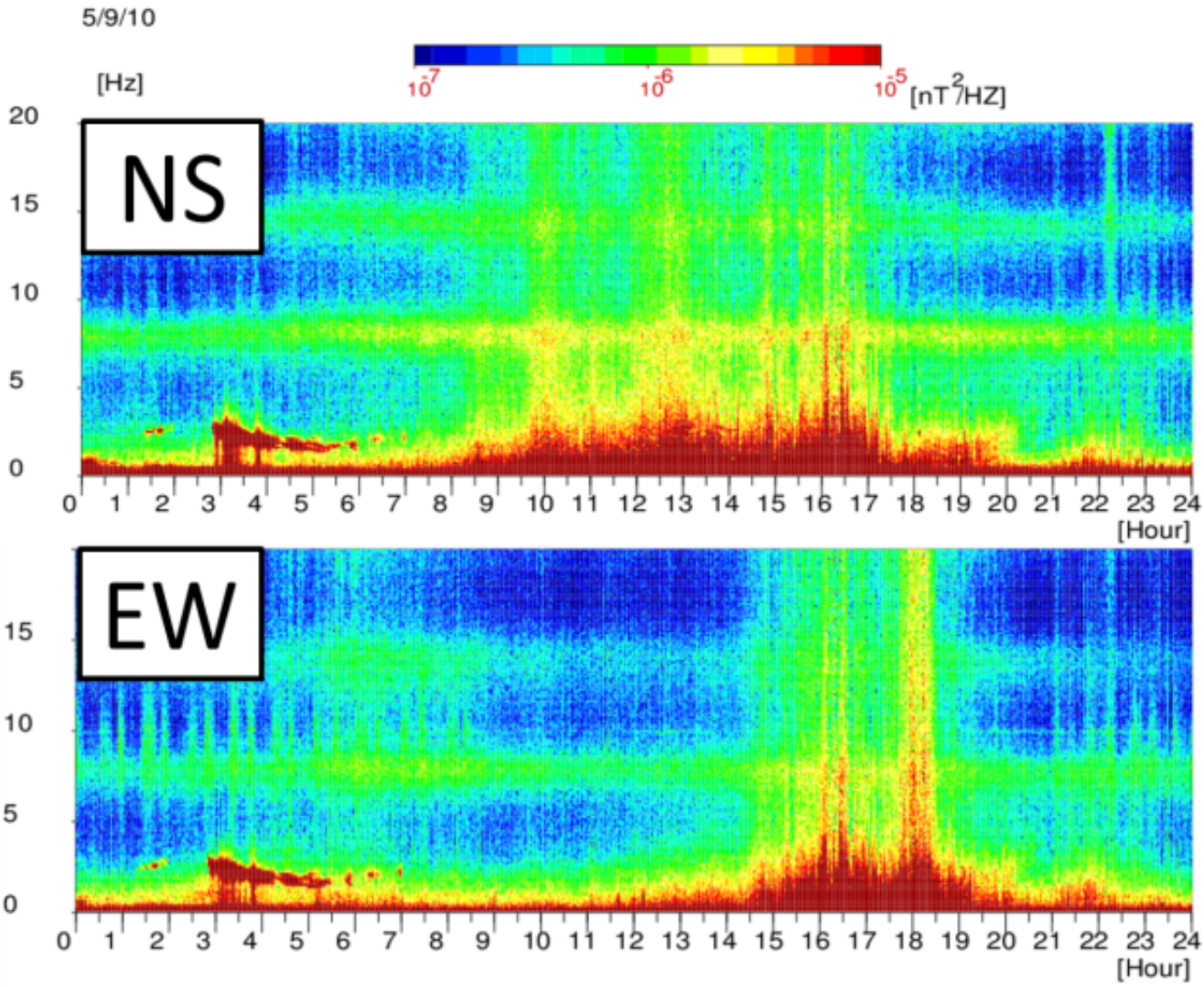

Low cost applications in astronomy, atmospheric science and communications using radio waves forward scattering from meteor trails

*Waleed Madkour[1], Masa-yuki Yamamoto[1]

1. Kochi University of Technology

The forward scattering of VHF radio signals by meteor ionized trails incorporates unique characteristics for usage in various applications. The oblique incidence of radio signals off the meteor trails enables the detection of fainter meteors using low-power transmitters. The relatively long duration of the scattered signals reflects the meteor trails behavior in relation to the atmospheric conditions near the meteor altitude region. It can also be used in communication of short bursts of data between distant locations on earth. In this research work, the usage of the forward scattering of radio waves by the meteor ionized trails in astronomy, upper atmospheric science and communication is presented. The developed meteor observation system follows the classical forward scattering setup commonly used worldwide. A methodology using locally developed software applications and interferometry technique to track the direction of each meteor echo is described as a fundamental step towards trajectory observations and hence meteor origins determination. Through using the same setup and software, the role of the secondary mesospheric ozone layer in oxidizing the meteor ionized trails was examined through meteor echoes duration distribution analysis during two meteor showers; the Perseids and the Geminids. Preliminary observations of the indirect link between solar cycle sun spot activity level and the meteor echo duration analysis is also presented. The observational research approach relies on extending the capabilities of the amateur basic setups by software automation in an attempt to fill the wide gap between the amateur systems and the professional ones. The gap that is mainly due to the difference in the amount of observational data each system can provide, can be partially filled through automation to provide enough data for statistical analysis. The methodology along with sample observational results for each application is described in detail as a proof of concept. The sample observational results in astronomy and upper atmospheric science applications are generally in agreement with the fundamentals of meteor science. Nevertheless, more statistical results are still required for further verification. In line with the observational activities, a practical meteor burst communication (MBC) study was performed to explore the feasibility of using modern technologies such as D-STAR ham-radio network and Android to simplify the MBC system. Although no positive results were obtained, the concept needs to be examined by higher power transmitters to compensate for the higher frequency used in the 144 MHz range. The three presented applications are not isolated from each other and the overlaps between them are highlighted. The low cost system setups introduced can be a model for low budget institutes planning to build a practical setup for educational as well as scientific purposes. The developed software applications are made free for use worldwide in order to support similar research themes.

Keywords: Meteor ionized trails, Radio Forward scatter, Interferometry

The development of software defined FMCW ionosonde based on the GNU Radio (2)

*Hiromitsu Ishibashi[1], Takuya Tsugawa[1], Takumi Kondo[1], Mamoru Ishii[1]

1. National Institute of Information and Communications Technology

We are developing a GNU Radio based software defined FMCW ionosonde system.
The initial result has been already presented at the SGEPSS 2016 fall meeting: as for the receiving system, we successfully got ionograms using the transmitting system of current FMCW ionosonde in Kokubuji and the
Ettus Research USRP N210. One of the main purposes of this work is to inherit peripheral units of current FMCW ionosonde system, which is currently operated in the Southeast Asia low-latitude ionospheric network (SEALION).
So, we have adopted X300 USRP instead of N210 and updated programs which is suitable for X300.
The additional frontend unit necessary to inherit peripheral units of current FMCW ionosonde system is being manufactured now.
This presentation is a subsequent follow-up report for these past 6 months.

Expansion of ionospheric TEC observation from measurements of single frequency GPS signals

*Yoshitaka Goto[1], Win Zaw Hein[1], Atsushi Matsui[1], Yoshiya Kasahara[1]

1. Graduate School of Natural Science and Technology

Monitoring of the ionospheric total electron content (TEC) using observational networks of GNSS signals is now popular in many countries. Most of the networks are built in mid latitude regions. It is important to expand them in low latitudes where many interesting phenomena of ionospheric plasma exist. The purpose of this study is to develop an estimation method of the ionospheric TEC using not multi-frequency receiver but single frequency ones, and expand an observation network in low latitude region at low costs.
Two observables are obtained from single frequency GPS measurements; code pseudorange and carrier phase. In these observables, the ionospheric effect appears plus and minus, respectively. The ionospheric effect is, then, derived by their difference while it includes a bias error. For the estimation of the bias error, the TEC distribution is assumed to be represented by two-dimensional (latitude-longitude) model with a polynomial function in each dimension. A thin layer model is assumed for altitude distribution of the ionospheric plasma. Ranging errors except for the ionospheric effect and receiver clock error in code pseudorange measurements are removed using precise ephemeris and existing appropriate models. Accuracy of the bias estimation is a few TECU that is equivalent to standard deviation of measurement error of the code pseudorange.
We are now planning to build continuous observation site in a low latitude region.

Keywords: Single frequency GPS signal, Ionospheric TEC, Bias estimation

N_2^+ resonant scattering light observation in the sunlit topside ionosphere with the auroral spectrograph

*Yu Endo[1], Takeshi Sakanoi[1], Yasunobu Ogawa[2], Masato Kagitani[1]

1. Planetary Plasma and Atomospheric Research Center, Graduate School of Science, Tohoku University, 2. National Institute of Polar Research

We report the ground-based optical remote-sensing of molecular ion upflow by measuring 427.8 nm N_2^+ resonant scattering in the sunlit topside ionosphere. *Störmer* [1955] has summarized his work on sunlit aurora from 1918 to 1943. He observed the sunlit aurora extending to 700-1100 km altitude and the strong emission from N_2^+. *Bates* [1949] suggested the N_2^+ emission at 427.8 nm is resonant scattering in the sunlit region. Recently, satellite data showed N_2^+ emission at the high altitude in the range from 400 to about 1,000 km. MSX satellite observed first the N_2^+ emission probably caused by N_2^+ upflow from the topside ionosphere [*Romick et al.*, 1999]. Ion upflow is essential for the source of ion outflow observed in the magnetosphere. O^+ ion upflow happens mainly during geomagneticaly disturbed conditions [*Moen et al.*, 2004, *Abe et al.*, 1993]. Furthermore, the heavier molecular ions which mainly exist in the E-region were also measured at about 10,000 km altitudes [*Yau et al.*, 1993]. However, the mechanism of these molecular ion upflow is uncertain. Now, we think that N_2^+ created by the charge exchange between N_2 and O^+ in F-region are upflowing during geomagnetically disturbed condition. Thus, we focus on N_2^+ 427.8 nm emission caused not by auroral precipitating electrons but by resonant scattering in the sunlit topside ionsphere associated with N_2^+ upflow using the data taken by Aurora Spectrograph (ASG) at Longyearbyen, Svalbard (geographic latitude : 75.2 deg and geographic longitude : 16:04 deg) for 13 years.

The ASG consists of a fish-eye lens, slit, grism and a cooled CCD detector which covers the wavelength range of 420-730 nm with a 2.0 nm spectral resolution and field of view of 180˚along the magnetic meridian. The ASG have been operating since 2000, but measuring N_2^+ emission 427.8 nm since 2004. The preceding study figured out that there is a high probability that the N_2^+ outflow occurs in geomagnetically disturbed condition (Kp > 4) [*Mizuno et al.*, 2005]. Therefore, we analyzed the 65 events during from 2004 to 2016 which the sun does not illuminate the ground and the Kp indices were greater than 4 for more than 9 hours. Then, if a single aurora arc appears in the geomagnetically southward direction, we can regard the auroral distribution as the auroral height profile. In this case, we can roughly assume the emission height with the simultaneous 557.7 and 630.0 nm emission. The oxygen emission at 557.7 nm is considered to be caused only by precipitating electrons, and if the 427.8 nm emission is distributed higher (larger elevation angle) than 557.7 nm, this 427.8 nm emission is resonant scattering light. We found 5 events in this cases of all 65 events. The Kp indices of these events are 4-, 2+, 3+, 4-, 6-, 5, and we found that there were two cases which are during geomagnetically disturbed conditions and not disturbed ones. Around 0700 UT on December 21, 2014 (Kp=2+), the maximum 427.8 nm emission is 400 R and Dst indice is -10 nT (an hour before the 427.8 nm observation). Then, the 427.8 nm emission peak is assumed to be at 380 km if the 630.0 nm emission peak is considered to be at 250 km. While, around 0100 UT on December 21, 2015, a geomagnetic storm occurred (Dst indice is -150 nT), and N_2^+ emission was observed at intensity of 800 R. Then, N_2^+ emission peak is 340 km and the emission at intensity more than 200 R extended up to 1,000 km and more. Of all 5 events, the N_2^+ emission peak is in 300~400 km in 4 events, the altitudes which the intensity are less than 200 R are higher increasing the activity of geomagnetism. This result suggests that N_2^+ is produced in the lower F-region and then upflowing with the geomagnetic activity. This is consistent with the preceding study.

Keywords: aurora, nitrogen molecular ion, up flow

Estimation of global scale airglow structure by observation from International Space Station

*Yusuke Kitamur[1], Akinori Saito[1], Takeshi Sakanoi[2], Yuichi Otsuka[3], Atsushi Yamazaki[4], Yuta Hozumi[1]

1. Department of Geophysics, Graduate School of Science, Kyoto University, 2. Planetary Plasma and Atmospheric Research Center, Graduate School of Science, Tohoku University, 3. Institute for Space-Earth Environmental Research, Nagoya University, 4. Institute of Space and Astronautical Science / Japan Aerospace Exploration Agency

We analyzed the dependence of large scale structure of night time airglow at 630 nm on the local time, latitude and longitude using ISS-IMAP/VISI observation data from the International Space Station and analyzed the IRI model TEC, IRI and MSIS airglow model .
ISS-IMAP/VISI is an airglow observer installed in the International Space Station for about 3 years from September 2012 to August 2015. It observes observes 630 nm airglow. At 630 nm, the airglow is emitting at around 250 km altitude, and the emission due to the equatorial anomaly has a dominant influence. We examined the dependence of 630nm airglow on local time, latitude and longitude, and compared it with the previous study. In the equator, it seemed that the latitude of the north and south became maximum at around 15 degrees due to equator anormaly. The equatorial anomaly weakened from the night to the morning and disappears, but it was observed that the observation was brightening around midnight and things like midnight temperature maximum were confirmed. Also, the asymmetry between the north and south hemisphere of the seasonal variation was confirmed. Similar asymmetry was observed in the 40 degrees north and south where the influence of equatorial anomaly was small.
In addition, we compared and verified the results of these results, total electron number data by IRI model which is an ionosphere model, and emission intensity of 630 nm airglow calculated from IRI model and MSIS model which is the atmosphere model.

Relationship between electron density height profile and convection flow speed in the polar cap patches and blobs

*Fukizawa Mizuki[1], Takeshi Sakanoi[1], Yasunobu Ogawa[2], Yoshimasa Tanaka[2], Keisuke Hosokawa[3], Satoshi Taguchi[4], Evan Thomas[5]

1. Planetary Plasma and Atmospheric Research Center, Graduate School of Science, Tohoku University, 2. National Institute of Polar Research, 3. Department of Communication Engineering and Informatics, University of Electro-Communications, 4. Department of Geophysics, Graduate School of Science, Kyoto University, 5. Dartmouth College

We focus on the enhanced electron density in the ionospheric F region associated with polar patches and blobs using the data taken with European Incoherent Scatter (EISCAT) radar and all-sky imager at Longyearbyen. Polar patches are regions of high-density plasma in the polar cap F-region. They are thought to be generated by expansion of the polar cap convection driven by pulsed reconnection [*Lockwood and Carlson*, 1992] and transported anti-sunward by $\boldsymbol{E}\times\boldsymbol{B}$ drift. Subsequently they exit polar cap and evolve into blobs in the sunward return flow region of closed field line. These phenomena play important role on electron density fluctuations in the polar cap and high-latitude ionosphere. However detailed processes controlling the electron density distribution are not understood well. EISCAT Svalvard Radar (ESR) observed the enhanced electron density in the F-region associated with polar patches 1730 to 2230 UT (2000-0100 MLT) on 11 January 2016. We interpreted that it is not caused by auroral electron precipitation because there is no enhanced electron density in the E-region and no enhanced ion temperature in the F-region. The direction of IMF was southward during 1530-1640 UT, 1730-1820 UT and 1930-2350 UT. Compared with the simultaneous OI (630.0 nm) emission all-sky images, eleven polar patches were identified. We find that the electron density profiles in the polar patches were classified into the two groups as follows: One is that electron density was enhanced in the altitude range from 300 to 500 km. The other is that the enhancement in electron density ranged from 250 to 350 km altitudes. On the other hand, SuparDARN data showed that the ion velocity in the polar cap in the latter case were higher than that in the former case. Thus, we suggest that this difference would be caused by the difference of ion convection speed in the polar cap as described in the following mechanism. When the ion velocity is high, the difference between the ion and neutral velocity becomes large and then the ion temperature increases by frictional heating. The increased ion temperature contributes to the growth of rate coefficients of $O^+ + N_2 \rightarrow NO^+ + O$ and $O^+ + O_2 \rightarrow O_2^+ + O$ reactions [*Schunk et al.*, 1976]. Consequently, electron density decreases by $NO^+ + e \rightarrow N + O$ and $O_2^+ + e \rightarrow O + O$ reactions. At high altitudes, NO^+ and O_2^+ density due to the enhanced NO^+ and O_2^+ scale heights with the increased ion temperature. Additionally, the successive electron density enhancements in the F region were observed by EISCAT Tromsø UHF Radar from 2037 to 2100 UT (2200 to 2230 MLT) on the same day. Simultaneous GPS-TEC map data indicates that it was probably caused by blobs in the closed field region originated from the polar cap. This interval was in the recovery phase of substorm according to AE index. Since the polar cap boundary shrinks in the substorm recovery phase, we suggest that Tromsø located into the sunward return flow region in the dusk convection cell, and then blobs passed over Tromsø.

Keywords: polar patch, blob

Statistical estimation of growth time of medium-scale traveling ionospheric disturbances by three dimensional spectral method

*Takafumi Ikeda[1], Akinori Saito[1]

1. Department of Geophysics, Graduate School of Science, Kyoto University

Medium scale traveling ionospheric disturbance is one of phenomenon in ionosphere and has been long studied. Nighttime MSTID will be caused by Perkins instability. Linear growth time(e folding time) of Perkins instability is very slow as growth time from random thermal noise . Therefore , we expect explanation of growth of MSTID by including electric filed of Sporadic E layer . However, we have not almost estimated observational growth time of MSTID.

Using this method, we statistically estimated growth rates of nighttime MSTID in japan in summer 2014 observed by GNSS. We used 3DFFT for total electron content(TEC) grid data ,and estimated propagation velocity. Using this velocity, we tracked movement of one wavefront of MSTID. We estimated the maximum growth time of each event by using wavenumber spectra when tracking. As a result, growth time is slower than 16 minutes. Propagation direction when growth time is fastest is southwestward(205˚ - 245˚). Growth time is maximum when 240˚. This magnitude is too slow as growth time of MSTID, and is within the range of one perkins instability expects. We will show the detail about the relation between this growth time and both mechanisms, and also show the solar activational and the seasonal dependence of growth time.

Keywords: Medium-scale traveling ionospheric disturbances, GPS-TEC, Perkins instability, Three dimensional spectral method

Role of gravity waves in the upper atmospheric temperature changes in association with sudden stratospheric warming

*Changsup Lee[1], In-Sun Song[1], Hwajin Choi[1], Jeong-Han Kim[1], Geonhwa Jee[1]

1. Korea Polar Research Institute

Fourier Transform Spectrometers (FTSs) at the Esrange space center (67°53′N, 21°04′E), Kiruna, Sweden and at the Dasan Korean Arctic station (78°55′N, 11°56′E), Svalbard, Norway have observed mesospheric air temperature from OH airglow emissions near 87 km height since November 2002. The FTS observations have provided simultaneous mesospheric temperature at the two different latitudes in association with elevated stratopause (ES) after major stratospheric sudden warming (SSW) events. ES-like phenomena and relevant warming have been simulated using global circulation models such as the whole-atmosphere community climate model (WACCM), but the model prediction is found to be much weaker mesospheric warming compared with the FTS and satellite observations especially in polar region such as the Dasan station. Considering that gravity waves (GWs) may have substantial impacts on the temperature and wind in the upper atmosphere, the discrepancy between observation and model may be attributed to common issues in GW parameterizations: Uncertainty in GW spectra and unrealism in GW propagation (i.e., columnar propagation). In this study, we investigate effects of the horizontal propagation and refraction of GWs on mesospheric warming associated with the ES after major SSW events using a ray-tracing model with specified GW spectra. Preliminary results for steady background flows show that the horizontal propagation and refraction increase westward GW momentum forcing near z = 100 km in the NH high latitudes that can induce downward motions and adiabatic warming in the NH polar regions below z = 100 km. Results are extended for time-varying background flows and different GW spectra to consider tidal effects and improve robustness of results, respectively.

Keywords: sudden stratospheric warming, gravity wave, ray tracing

Spatial Distributions of Total Electron Content Variations Associated with Earthquakes

Shun Shomura[1], *Hiroyuki Nakata[1], Hiroyo Ohya[1], Toshiaki Takano[1], Takuya Tsugawa[2], Michi Nishioka[2]

1. Graduate School of Engineering, Chiba University, 2. National Institute of Information and Communications Technology

The coseismic ionospheric disturbances are generated by the acoustic wave and atmospheric gravity wave excited by earthquakes. In the previous studies, it is found that the perturbations of total electron content (TEC) are correlated with the magnitude of the earthquake. On the other hand, the relationship between the magnitude and the spatial distributions of these perturbations are not examined in detail. Using two-dimensional TEC maps derived from the GNSS Earth Observation Network (GEONET), in this study, we have analyzed the spatial distributions of TEC variations associated with earthquakes. First of all, the TEC distribution map is divided in grid whose size is 0.2 x 0.2 degrees. The spectral intensity of the TEC perturbations is calculated using Fast Fourier Transform. The average of the spectral intensity in each grid is determined from those in the ionospheric pierce points (altitude = 350 km) located with in each grids. After the center of the TEC variation distributions are determined from the average map, the latitudinal and longitudinal width of the TEC perturbations are estimated by fitting the perturbations with the Gaussian function. We analyzed 5 earthquakes (M > 6.8) whose epicenters are located at the sea around Japan since 2000. The wave recorders installed by the Japan Meteorological Agency observed the heights of tsunamis. Using these data, the heights of tsunamis in the epicenter are determined using Green's theorem, which explains the relationship between the height of tsunami and the depth of the sea. The results of the fitting shows that the latitudinal width of TEC variations is correlated with the height of tsunami, while longitudinal one is not. This is because, in the events that occurred along the coast, the height of tsunami is highly fluctuated due to the coast line. In such events, therefore, we determined the latitudinal width of TEC variations using ionospheric pierce points located on land-side. In the result, the correlation between the longitudinal distribution of TEC variations and the height of tsunami increased. Since the correlation between TEC variations and the height of tsunami is high, if events of the analysis target increase in the future, there is a possibility that the location, time and scale of the tsunami can be estimated.

Keywords: Total Electron Content, Earthquake

Improvement of high-latitude electric field model in GAIA

*Chihiro Tao[1], Hidekatsu Jin[1], Hiroyuki Shinagawa[1], Yasunobu Miyoshi[2], Hitoshi Fujiwara[3], Mitsuru Matsumura[4]

1. National Institute of Information and Communications Technology, 2. Kyushu University, 3. Seikei University, 4. Institute for Space-Earth environmental Research, Nagoya University

GAIA (Ground-to-Topside Model of Atmosphere and Ionosphere for Aeronomy) solves physical and chemical dynamics of the whole atmosphere region from the troposphere to the exosphere under interactions with the ionosphere. Input from the polar region dramatically varies depending on the solar wind and magnetospheric conditions, which affects thermosphere and ionosphere globally. Total electron contents around Japan show discrepancy between observation and GAIA simulation without the polar input variation especially disturbed term. We are conducting improvement of the polar electric field input to GAIA referring to an empirical Weimer model which varies as a function of solar wind parameters. We will report the development and initial results in this presentation.

Keywords: thermosphere, ionosphere, simulation

